

Curriculum learning for annotation-efficient medical image analysis: scheduling data with prior knowledge and uncertainty

Amelia Jiménez-Sánchez, Diana Mateus, Sonja Kirchhoff, Chlodwig Kirchhoff, Peter Biberthaler, Nassir Navab, Miguel A. González Ballester, Gemma Piella

Abstract—Convolutional neural networks (CNNs) for multi-class classification require training on large, representative, and high quality annotated datasets. However, in the field of medical imaging, data and annotations are both difficult and expensive to acquire. Moreover, they frequently suffer from highly imbalanced distributions, and potentially noisy labels due to intra- or inter-expert disagreement. To deal with such challenges, we propose a unified curriculum learning framework to schedule the order and pace of the training samples presented to the optimizer. Our novel framework reunites three strategies consisting of individually weighting training samples, reordering the training set, or sampling subsets of data. The core of these strategies is a scoring function ranking the training samples according to either difficulty or uncertainty. We define the scoring function from domain-specific prior knowledge or by directly measuring the uncertainty in the predictions. We perform a variety of experiments with a clinical dataset for the multi-class classification of proximal femur fractures and the publicly available MNIST dataset. Our results show that the sequence and weight of the training samples play an important role in the optimization process of CNNs. Proximal femur fracture classification is improved up to the performance of experienced trauma surgeons. We further demonstrate the benefits of our unified curriculum learning method for three controlled and challenging digit recognition scenarios: with limited amounts of data, under class-imbalance, and in the presence of label noise.

Index Terms—curriculum learning, self-paced learning, data scheduler, multi-class classification, limited data, class-imbalance, noisy labels

I. INTRODUCTION

CONVOLUTIONAL neural networks (CNNs) are nowadays the model of predilection for computer-aided diagnosis (CAD). They have been rapidly integrated in numerous medical applications [1]–[5] due to their strong capacity to learn, directly from data, meaningful and hierarchical image representations. However, their feature extraction ability heavily depends not only on the optimization scheme but also on the training dataset. To be properly trained, CNNs need a large dataset representative of the population of interest [6].

In medical image analysis tasks, under the supervised learning paradigm, acquiring reliable and clinically relevant annotated (*a.k.a.* labeled) data remains a key challenge. Typically, manual annotations call for the time and effort of clinical experts such as radiologists or pathologists. Even when expert annotations are available, intra- or inter-expert disagreement may lead to unreliable labels. In addition, medical datasets usually suffer from class imbalance due to difficulties in collecting cases and the incidence of rare diseases. Finally, medical image data needs also dealing with proprietary and/or privacy concerns. As a result, these datasets generally exhibit three main challenging characteristics: (i) limited amounts of data, (ii) class-imbalance, and (iii) uncertain annotations. The most common approaches to alleviate these challenges have been transfer learning [1], [4], [7], [8], data augmentation [9] and semi-supervised learning [8], [10]. More recently, the attention has been shifted towards bootstrapping or weighting strategies [11], sample mining [12], active learning [13], and curriculum learning [14]–[17].

The underlying intuition of some of the latter methods is that strategies like weighting, selecting or simply ordering the samples can significantly impact the optimization during training. Towards this objective, we propose a unified curriculum learning (CL) approach reuniting the above strategies to improve the performance of multi-class classification CNNs, by dealing with the lack of large annotated datasets, class imbalance, and annotation uncertainty. Inspired by the concept of curriculum in human learning, CL presents the training samples to the algorithm in a meaningful order (often by

Submitted on 31st July 2020. This project has received funding from the European Unions Horizon 2020 research and innovation programme under the Marie Skłodowska-Curie grant agreement No. 713673 and by the Spanish Ministry of Economy [MDM-2015-0502]. A. Jiménez-Sánchez has received financial support through the “la Caixa” Foundation (ID Q5850017D), fellowship code: LCF/BQ/IN17/11620013. D. Mateus has received funding from Nantes Métropole and the European Regional Development, Pays de la Loire, under the Connect Talent scheme. Authors thank Nvidia for the donation of a GPU.

A. JS., G. P., and M. A. G. B. are with BCN MedTech, Department of Information and Communication Technologies, Universitat Pompeu Fabra, 08018 Barcelona, Spain. (e-mails: amelia.jimenez@upf.edu, gemma.piella@upf.edu, ma.gonzalez@upf.edu). M. A. G. B. is also with ICREA, Barcelona, Spain.

D. M. is with Ecole Centrale de Nantes, LS2N, UMR CNRS 6004, 44321, Nantes, France (e-mail: diana.mateus@ec-nantes.fr).

S. K., C. K., P. B. are with Department of Trauma Surgery, Klinikum rechts der Isar, Technische Universität München, 81675, Munich, Germany (e-mail: sonja.kirchhoff@me.com, dr.kirchhoff@me.com, peter.biberthaler@mri.tum.de). S. K. is also with Institute of Clinical Radiology, LMU München, Munich, Germany.

N. N. is with Computer Aided Medical Procedures, Technische Universität München, 85748, Munich, Germany (e-mail: nasir.navab@tum.de). N. N. is also with Johns Hopkins University, 21218, Baltimore, USA.

difficulty from “easy” to “hard”) and has been shown to avoid bad local minima and lead to an improved generalization [18]. The ordering can be either fixed (*e.g.* set heuristically by a “teacher” or domain-specific knowledge) or, in the absence of a-priori knowledge, a self-paced order [19] derived from the algorithm’s performance (*e.g.* the loss). Our unified CL framework encompasses both approaches. Finally, we address the lack of prior knowledge to design an ad-hoc curriculum, by providing a ranking criterion based on uncertainty modelling.

In practice, our framework incorporates three manners to actually implement the curriculum data sequencing. The first one is based on reordering the training set. The second uses a sampling strategy, *i.e.* selecting increasingly growing subsets. The last one employs a weighting scheme to give different importance to the training samples.

Lately, training CNNs with ordered sequences has been shown to improve medical image segmentation by gradually increasing the context around the areas of interest [20]–[22]. To the best of our knowledge, only few works have explored sample reordering for CAD with CNN, for instance by extracting prior knowledge from radiology reports [14] or medical guidelines [17].

To show the impact of our proposed method, we perform two types of experiments. First, on the MNIST dataset as a controlled environment. Then, we evaluate the method on a real application that presents the three types of addressed challenges, namely, proximal femur fracture classification. This multi-class problem is inherently imbalanced, as the frequency of the classes reflects their incidence. Moreover, the adequate classification takes several years of daily clinical routine in the trauma surgery department, limiting the collection of annotations and leading to potentially noisy labels¹.

Contributions: In this work, we propose a unified CL framework to automatically schedule the order and pace of the training samples for an improved multi-class classification. Our contributions are:

- We identify the common elements among different data scheduling strategies and present them within a unified framework. We examine their behaviour and analyze their performance under different data challenges.
- We propose two types of ranking functions allowing to prioritize training data: one according to prior-knowledge, and a second one measuring the prediction’s uncertainty according to the model’s performance.
- With a controlled experimental setting, we confirm that all the variants are useful in reducing the classification error under limited amounts of data, imbalance in the class distribution, and unreliable annotations.
- We validate the method for the classification of proximal femur fractures and show that these improvements also extend to real medical datasets.

This paper is structured as follows. Section II covers CL related works that are relevant for the design of data schedulers. In Section III, the details of our proposed framework are presented. Section IV describes the specifications of the

experimental validation. Section V shows the classification performance. Section VI discusses our findings, recommendations and future work. Finally, Section VII summarizes our conclusions.

II. RELATED WORK

Recently, CL, self-paced learning (SPL), active learning (AL) and selection strategies have been studied to deal with the mentioned medical data challenges. These methods rely on ranking the learning samples. Several criteria have been used for ranking, among which we highlight the two included in our framework: (i) domain-specific prior knowledge and (ii) data and model uncertainty.

Prior knowledge is leveraged in [14]–[17] to design a curriculum for classification. Yang *et al.* [15] exploited SPL to handle class-imbalance, by combining the number of samples in each class and the difficulty of the samples, which is derived from the loss. Tang *et al.* [14] proposed to feed the images in order of difficulty based on severity-levels mined from radiology reports to improve the localization and classification of thoracic diseases. Jiménez-Sánchez *et al.* [17] exploited the knowledge of the inconsistencies in the annotations of multiple experts and medical decision trees, to design a medical-based deep curriculum that boosted the classification of proximal femur fractures. Trying to mimic the training of radiologists, Maicas *et al.* [16] proposed to pretrain a CNN model with increasingly difficult tasks, before training for breast screening. The pretraining tasks were selected using teacher-student CL, that samples tasks that can achieve a higher improvement on their performance. In this work, we schedule our training data based on a scoring function that ranks the samples according to domain-specific prior knowledge. Different from previous works, we encompass several scheduling strategies, namely reordering the training set, subset sampling, and weighting within a unified framework.

The second criterion that we consider for defining a curriculum is uncertainty. The estimation of uncertainty provides a way of systematically defining the difficulty of the samples. Xue *et al.* [12] proposed online sample mining based on uncertainty to handle noisy labels in skin lesion classification. In their work, uncertainty is approximated through the classification loss. However, the most common methods for estimating classification uncertainty, in the context of deep learning, rely on Bayesian estimation theory, namely using Monte-Carlo (MC) dropout [24]. Uncertainty is probably the most frequent criterion in active learning selection strategies. Recently, Wu *et al.* [25] combined uncertainty together with image noise into their active learning scheme to alleviate medical image annotation efforts. Uncertainty and label correlation are integrated in the sampling process to determine the most informative examples for annotation. Active learning pays attention to examples near the decision surface to infer their labels. Similarly, we aim to gradually move the classification decision border by adding examples of increasing ranking scores. We prioritize in our second scoring function the most representative samples, letting uncertainty guide their order, pace or weight.

¹Inter-reader agreement, for the classification of proximal femur fractures according to the AO system, ranges between 66-71% [23].

We validate the proposed framework for the classification of proximal femur fractures. Whereas most of the previous work on femur fractures focuses on the binary fracture detection task [26]–[28], we target the more challenging multi-class classification according to the AO standard [17], [29], [30].

Approaches to boost fracture classification accuracy comprise prior localization or transfer learning. The localization of a region of interest before the classification of the full image has been studied either in a weakly-supervised [28], [29] or in a supervised [30] way. Knowledge transfer has been investigated across image domains, *i.e.* using ImageNet dataset for pretraining [26], [31], and across tasks, *i.e.* training first on body part detection (easier task) and then focusing on the hip fracture detection [27].

In our previous work [17], a series of heuristics, based on knowledge such as medical decision trees and inconsistencies in the annotations of multiple experts, were proposed to boost fracture classification performance. Here, we propose a more general unified CL framework that includes our previous work, and also provides an alternative mechanism, based on prediction uncertainty, in case prior knowledge is unavailable.

III. METHOD

Given a multiclass image classification task, where an image x_i needs to be assigned to a discrete class label $y_i \in \{1, \dots, T\}$, our training set is defined as $X = \{(x_1, y_1), \dots, (x_N, y_N)\}$. Before prediction, a CNN model h with parameters θ is trained with stochastic gradient descent. Training samples are typically randomly ordered. Our goal is to schedule the order and pace of the training data presented to the optimizer to better exploit the available data and annotations, and thereby improve the classification performance.

To learn the best CNN model h_{θ^*} from the input data, a common choice is to use empirical risk minimization:

$$\mathcal{L}(\theta) = \mathbb{E}[L_\theta] = \frac{1}{N} \sum_{i=1}^N L_\theta(x_i, y_i) \quad (1)$$

$$\theta^* = \arg \min_{\theta} \mathcal{L}(\theta)$$

where L_θ is the loss function that measures the cost of predicting $h_\theta(x_i)$ when the correct label is y_i .

Optimization is conducted with stochastic gradient descent for a total of E epochs. Typically, the objective function L_θ is non-convex and is minimized in mini-batches of size B . Therefore, different ordering of the training samples may often lead to different local minima. We can rewrite Eq. (1) as:

$$\mathcal{L}(\theta) = \frac{1}{N} \sum_{j=1}^{N/B} \sum_{i=1}^B L_\theta(\hat{x}_{i,j}, \hat{y}_{i,j}), \quad (2)$$

where $\hat{x}_{i,j}$ is the i -th sample in the j -th batch, $\hat{x}_{i,j} = x_{i+(j-1) \cdot B}$, and $\hat{y}_{i,j}$ is the corresponding label.

We propose to modify Eq. (2) to schedule the data. To do so, first, we introduce the different components required for reordering, pacing and weighting the training data in Subsection III-A. Then, in Subsection III-B, we formalize two types of scoring functions to assign a priority to each data sample according to domain-specific prior knowledge or the

samples' uncertainty measured with MC dropout. Finally, we cover the implementation details of the three variants of our unified CL method in Subsection III-C.

A. Data scheduler

In the following, we define the scheduling elements required for reordering and pacing our training data: a scoring function s , curriculum probabilities p , a permutation function π , a pacing function g and a weighting function α . The data scheduler takes as input the training set X , the scoring and pacing functions, s and g , respectively, and it outputs the reordered set/subset, then partitioned in mini-batches. All components are updated at each epoch e .

- The *scoring function* $s : \mathcal{X} \rightarrow \mathbb{R}$ ranks the curriculum priority of each training pair. The curriculum priority can take various forms, such as difficulty or prediction disagreement. Then, an example (x_i, y_i) has higher priority than example (x_j, y_j) if $s(x_i, y_i) > s(x_j, y_j)$. We define $s_i = s(x_i, y_i)$ and, in an abuse of notation, use s to denote both the scoring function and the vector (s_1, \dots, s_N) .
- The *curriculum probabilities* p are obtained by normalizing the score function values to $[0, 1]$ range. For example, one can choose $p_i = s_i / \|s\|_1$, assuming $s_i \geq 0$. So that a pair (x_i, y_i) is more likely to be presented earlier to the optimizer than a pair (x_j, y_j) if $p_i > p_j$.
- The *reordering function* $\pi : [1, \dots, N] \rightarrow [1, \dots, N]$ is a permutation. It is determined by resampling X (without replacement) according to the curriculum probabilities p .
- The *pacing function* $g : \mathbb{N} \rightarrow \mathbb{N}$ controls the learning speed by presenting growing subsets of data. The batch size B is kept fixed. The mapping g determines the subset size $N_S \leq N$ at each training epoch e , *i.e.* $g(e) = N_S^{(e)}$.
- The *weighting function* $\alpha : \mathcal{X} \rightarrow \mathbb{R}$ favors the samples that have higher priority according to the curriculum probabilities. These weights are applied directly to the classification loss.

Taking into account the scheduling elements introduced, we can rewrite the optimization loss at epoch e for our unified CL framework as:

$$L_\theta^{(e)} = \frac{1}{N_S^{(e)}} \sum_{j=1}^{N_S^{(e)}/B} \sum_{i=1}^B \hat{\alpha}_{i,j}^{(e)} L_\theta(\hat{x}_{i,j}^{(e)}, \hat{y}_{i,j}^{(e)}), \quad (3)$$

where $\hat{x}_{i,j}^{(e)} = x_{\pi^{(e)}(i+(j-1) \cdot B)}$ corresponds to the i -th sample from the j -th batch at epoch e after reordering π . The same relation follows for its corresponding label and weight, $\hat{y}_{i,j}^{(e)}$ and $\hat{\alpha}_{i,j}^{(e)}$, respectively. We will drop superscript (e) when no confusion arises. Also, we simplify notation and use x_i (and y_i , α_i) to refer to a given (already reordered) sample (and label, weight).

B. Scoring function definition

The key element of our approach is the definition of the scoring function or, equivalently, the curriculum probabilities p , which allow us to sample the dataset and obtain the reordering function π that schedules the training samples. In

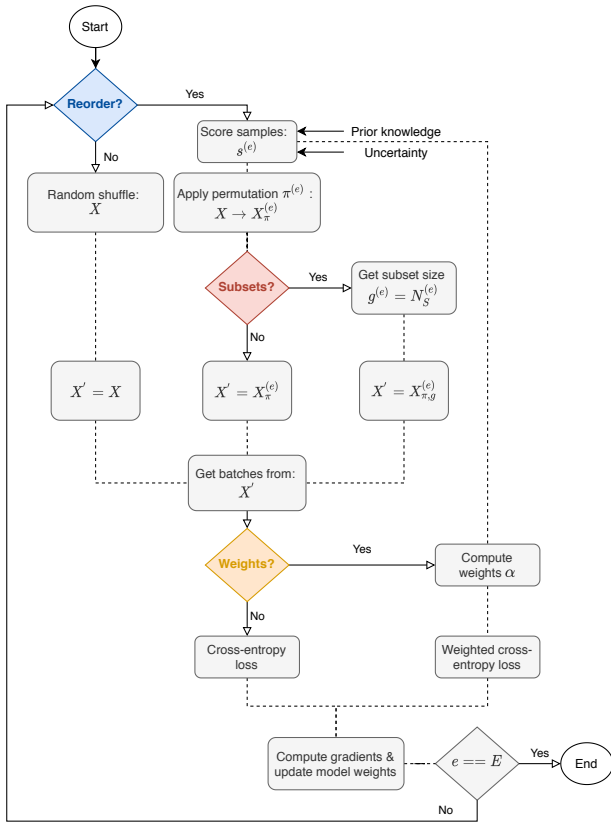


Fig. 1: Diagram illustrating the components of the proposed unified CL method reuniting the three scheduling strategies: reorder, subsets and weights.

this subsection, we present two alternative scoring functions. The first one is static and based on some initial (domain) knowledge, as in classical CL [18]. The second one is dynamic and based on the estimation of uncertainty, inspired by SPL [19], [33].

1) Prior knowledge: In this scenario, the initial scoring $s^{(0)}$ and, thus, curriculum probabilities $p^{(0)}$, are specified based on domain prior knowledge. We assume in this work that the scoring values are defined per class:

$$s^{(0)}(\cdot, y_i = t) = \omega_t, \quad (4)$$

where $t \in \{1, \dots, T\}$ serves as index of the classes. ω_t is defined specifically for each task (or dataset). Once that the scoring values have been initialized, they can be kept fixed or decayed towards a uniform distribution [18]. In either case, as the curriculum probabilities are predetermined a priori in Eq. (4), we refer to this approach as static CL.

Prior knowledge can be obtained, for example, extracting keywords from medical reports [14], based on the frequency of samples [15], [17], employing medical classification standards or quantifying inconsistencies in the annotations [17]. Specifically for this work, we define the initial probabilities for the proximal femur fracture images based on Cohen's kappa [34]. This statistic is used to measure the agreement of clinical experts on the classification between two readings. Basically, the kappa coefficient quantifies the ratio between the observed and chance agreement. For digit recognition,

we extract prior knowledge by ranking the per-class F_1 -score performance after few epochs of training. The exact values used for our experiments are specified in Subsection IV-B.

2) Uncertainty estimation: In absence of domain knowledge, we propose to estimate the priority of the training samples by dynamically quantifying the uncertainty of the model predictions. Uncertainty provides a way of systematically ranking the training samples based on the model's agreement on the predictions, without requiring any prior knowledge. We compute and use the uncertainty estimation at each epoch e in predicting a sample x_i as its scoring value s_i . The goal is to emphasize samples with high information gain at early stages of training, *i.e.* to rapidly reduce the error in highly-misleading samples.

To estimate the uncertainty of the model predictions, we employ MC dropout [24]. In this training regime, each epoch includes two stages [35]: uncertainty estimation and label prediction. In the uncertainty estimation stage, we perform K stochastic forward passes on the model under random dropout. The K estimators are used to measure the uncertainty of the output of the model. In the prediction stage, a single forward pass is performed. Then, the classification loss is used to measure the difference between the prediction and the label.

Let $\sigma \in \mathbb{R}^T$ be the (softmax) output of the CNN. This output represents the probability distribution of the predicted label over the set of the possible classes for sample x , *i.e.*, $P(y = t | x, \theta) := \sigma_t$. We measure uncertainty as the entropy [36] of the output distribution, *i.e.* predictive entropy:

$$H(y|x, \theta) = - \sum_{t=1}^T P(y = t | x, \theta) \cdot \log P(y = t | x, \theta). \quad (5)$$

The output distribution $P(y = t|x, \theta)$ can be approximated using MC integration:

$$\tilde{P}(y = t | x, \theta) = \frac{1}{K} \sum_{k=1}^K P(y = t | x, \theta_k), \quad (6)$$

where $P(y = t | x, \theta_k)$ is the probability of input x to take class t with model parameters $\theta_k \sim q(\theta)$, with $q(\theta)$ being the (dropout) variational distribution. We set the scoring function to be the estimated predictive entropy, computed from the MC estimated output distribution $\tilde{\sigma}_t = \tilde{P}(y = t | x, \theta)$:

$$s = - \sum_{t=1}^T \tilde{\sigma}_t \cdot \log \tilde{\sigma}_t. \quad (7)$$

By assigning low scoring values to predictions with low predictive entropy, we reduce/decrease the priority of samples with low information gain. Note that in contrast with Eq. (4), here, the scoring vector s is defined independently for each sample, and updated after each epoch. Only few works measure uncertainty while learning the classification task [37]. To the best of our knowledge, our proposed dynamic uncertainty-driven strategy is novel for CAD.

C. Scheduling data with curriculum learning

In practice, any curriculum is implemented by assigning a predefined or estimated probability p_i to each training pair

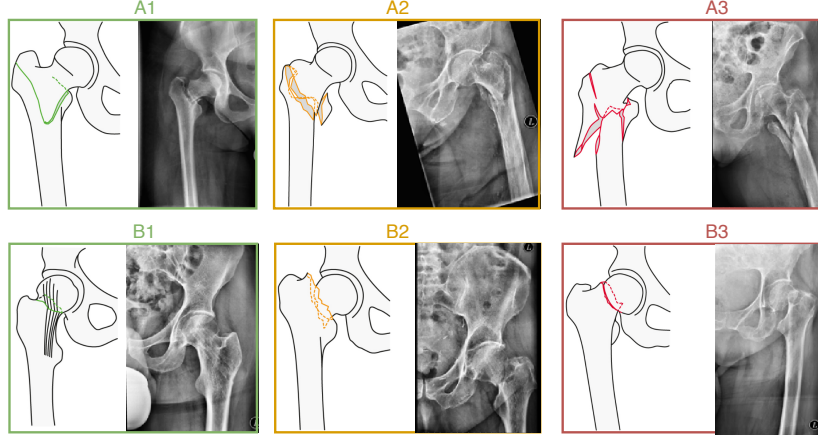


Fig. 2: Examples of proximal femur fractures and their fine-grained AO classification, adapted from [32].

(x_i, y_i) , as described in Subsection III-B. We integrate in our framework three main ideas from the literature, to exploit the probabilities during the optimization. Each of them is depicted by a diamond shape in Fig. 1.

The first mechanism, *reorder*, presents the samples to the optimizer in a “smart” probabilistic order, instead of the typical random permutation. This strategy aims to deal with low-priority cases at a later stage of training [17], [18], [38]. At the beginning of every epoch e , the training set $X = \{(x_1, y_1), \dots, (x_N, y_N)\}$ is permuted to $X_\pi^{(e)} = \{(x_{\pi^{(e)}(1)}, y_{\pi^{(e)}(1)}), \dots, (x_{\pi^{(e)}(N)}, y_{\pi^{(e)}(N)})\}$ using the reordering function $\pi^{(e)}$. This mapping results from sampling, without replacement, the training set according to the curriculum probabilities $p^{(e)}$ at the current epoch e . Mini-batches are formed from $X_\pi^{(e)}$.

The second method, *subsets*, builds upon the reordered training set and selects gradually increasing subsets at every epoch. The purpose is to reduce the effect of outliers at the beginning of training [12], [33], [38]. Mini-batches are obtained from $X_{\pi, g}^{(e)} \subseteq X$, where $X_{\pi, g}^{(e)}$ are the first $N_S^{(e)}$ pairs of $X_\pi^{(e)}$. The subset size at every epoch $N_S^{(e)}$ is determined by the pacing function g . Initially, it is set to a predefined portion of the training set $N_S^{(0)}$. For simplicity, in our experiments we choose g to be a staircase function:

$$g(e) = N_S^{(e)} = \begin{cases} N_S^{(0)} + e \cdot \Delta & \text{if } 1 \leq e < E_S \\ N & \text{if } e \geq E_S \end{cases} \quad (8)$$

where $\Delta = (N - N_S^{(0)})/E_S$ and E_S is the number of epochs before considering the whole training set.

A counter τ_i is introduced to track the selected pairs. Their scoring vector is decreased, thus favoring new pairs in the subsequent epoch. We choose to update the scoring vector using an exponential decay:

$$s_i^{(e)} = s_i^{(e-1)} \cdot \exp(-\tau_i^2/10) \quad e = 1, \dots, E. \quad (9)$$

The third approach, *weights*, assigns scalar weights to training samples based on their curriculum probabilities [33]. We propose to individually weight the training samples in the classification loss L_θ in Eq. (3), in the form of a weighted

cross-entropy loss. The role of the weights is to decrease the contribution to the classification loss of samples with low priority. We choose the weights $\hat{\alpha}_{i,j}$ to correspond to a per-batch normalization of the curriculum probabilities:

$$\hat{\alpha}_{i,j}^{(e)} = \frac{p_{i+(j-1) \cdot B}^{(e)}}{\max_k p_{k+(j-1) \cdot B}^{(e)}} = \frac{\hat{p}_{i,j}^{(e)}}{\max_k \hat{p}_{k,j}^{(e)}}. \quad (10)$$

When the curriculum is driven by uncertainty, the resulting approach is similar to boosting [39]. In the boosting method, misclassified examples are given a higher weight than correctly classified ones. This is known as “re-weighting”. Following the same principle, we use the uncertainty at every epoch to update the values of the weights.

IV. EXPERIMENTAL VALIDATION

In order to validate the positive effect of data scheduling on the classification performance, we perform experiments on two types of image databases: (i) a real in-house dataset of a moderate size and naturally suffering from imbalance and noisy labels, and (ii) the MNIST dataset. The second one is used for further analysis under controlled experiments.

A. Datasets

Proximal femur fractures: Our clinical dataset consists of anonymized X-rays of the hip and pelvis collected at the trauma surgery department of the Rechts der Isar Hospital in Munich. The collection of these radiographs was approved by the ethical committee of the Faculty of Medicine from the Technical University of Munich, under the number 409/15 S. The dataset consists of 327 type-A, 453 type-B fractures and 567 non-fracture cases. Class labels were assigned by clinical experts according to the AO classification standard [32]. This standard follows a hierarchy according to the location and configuration of the fracture lines. Fractures of type-A are located in the trochanteric region, and fractures of type-B are those affecting the area around the femur neck. Each type of fracture is further divided into 3 subclasses depending on the morphology and number of fragments of the fracture, see Fig. 2. Subtypes of the fracture classes are highly unbalanced,

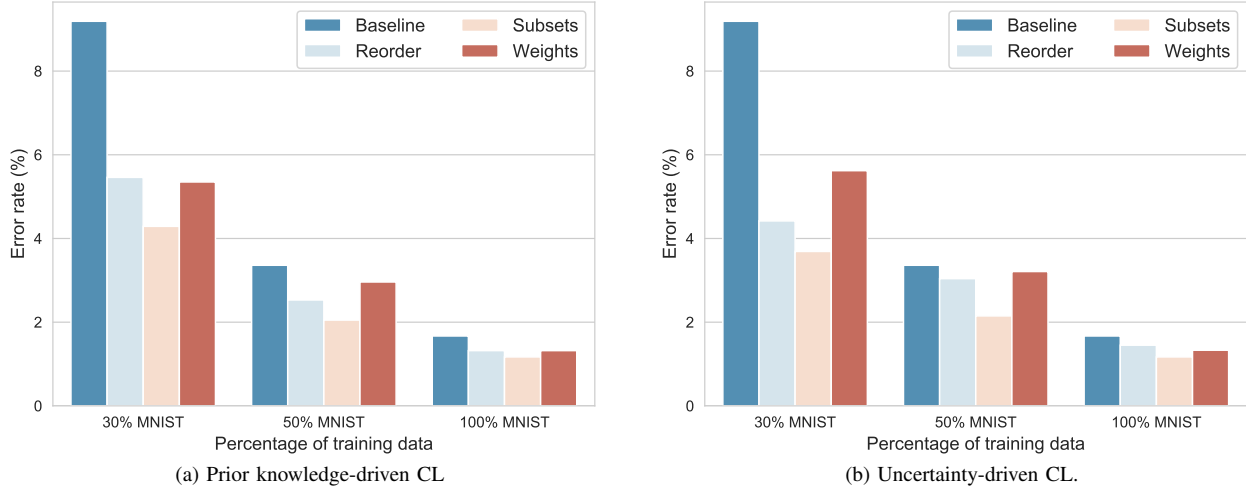


Fig. 3: Classification performance for digit recognition,. The proposed curriculum method reduces the baseline error rate in all variants under limited amounts of data.

reflecting the incidence of the different fracture types [17]. The dataset was split patient-wise into three parts with the ratio 70%:10%:20% to build respectively the training, validation and test sets. We evaluate the classification performance of the 3-class (type-A or type-B and non-fracture) and 7-class (fracture subtypes and non-fracture) classification tasks. The test distribution was balanced between fracture type-A, type-B, and non-fracture cases.

MNIST: The MNIST handwritten digit database is publicly available². It has a training set of 50000 examples and a validation and test sets of 10000 examples each. Classes are equally represented.

B. Implementation details

Architectures and optimization hyperparameters: We train our models 10 times for 30 epochs, with an early stopping criterion of no improvement in the validation set for 20 epochs. For the digit recognition task, we use an upgraded ConvPool-CNN-C [40] proposed by [41]. This architecture replaces pooling layers by convolutional layers with a stride of two. Besides, the small convolutional kernels greatly reduce the number of parameters of the network. It yielded competitive performance on several object recognition datasets (CIFAR-10, CIFAR-100, ImageNet). For the fracture classification, we deploy a ResNet-50 [42] pretrained on the ImageNet dataset, on account of the limited size of our dataset and the benefits of transfer learning [1], [8]. Our CNNs are trained with stochastic gradient descent and a momentum of 0.9. The initial learning rate is set to $1e-3$, and decayed by a factor of 10 every 10 epochs. We use a mini-batch size of 64 and a dropout rate for the fully connected layer of 0.9 (0.7 for uncertainty estimation). For the subsets strategy, the warm-up epochs hyperparameter E_S in Eq. (8) is set to 10 and the initial subset size $N_S^{(0)}$ to 25% of the training data at each scenario.

Prior knowledge:

- Proximal femur fractures. In this setting, we leverage, as prior knowledge the intra-reader agreement from a committee of experts: a trauma surgery attendant with one year experience, a trauma surgery attending and a senior radiologist [43]. The scoring values for the seven classes are the following:

$$\omega = (0.69, 0.56, 0.62, 0.60, 0.56, 0.38, 0.92). \quad (11)$$

These values correspond to the multi-read kappa agreement described in Results section [43].

- MNIST. In absence of domain-specific knowledge, a CNN is trained for 5 epochs. After observing the F_1 -score of each of the classes, weights are assigned, by ranking the classes from easiest (highest F_1 -score) to hardest (lowest F_1 -score). Then, training is restarted from scratch using these particular weights. We specify the values for the experiments with limited amounts of data $\omega_{limited}$, under class-imbalance $\omega_{imbalance}$, and with noisy/corrupted labels ω_{noise} :

$$\omega_{limited} = (7, 10, 5, 4, 9, 1, 8, 6, 2, 3) \quad (12)$$

$$\omega_{imbalance} = (3, 10, 7, 8, 5, 6, 9, 4, 1, 2) \quad (13)$$

$$\omega_{noise} = (8, 10, 9, 7, 5, 1, 2, 3, 4, 6). \quad (14)$$

Experimental setting: We perform a comparative evaluation of the classification task with five series of experiments. Our method is contrasted against its “anti-” approach, *i.e.* the curriculum probabilities are complemented, “random” criterion, *i.e.* the curriculum probabilities are assigned randomly, and the “baseline” model. The latter does not consider any data scheduling.

In the first series of experiments, we examine the performance of our method driven by prior knowledge. In the second series, we consider the use of uncertainty to overcome the lack of prior knowledge. Our clinical dataset inherently suffers from class-imbalance, unreliable annotations and a limited

²<http://yann.lecun.com/exdb/mnist/>

TABLE I: Digit classification results over 10 runs: mean error rate (%). The highlighted values in bold correspond to the best metric per curriculum method. The underlined values correspond to the best metric per scenario, *i.e.* percentage of data.

| Prior knowledge | Baseline | Reorder | | Subsets | | | Weights | | |
|-----------------|----------|---------|-------------|---------|---------|-------------|---------|---------|-------------|
| | | Anti-CL | CL | Random | Anti-CL | CL | Random | Anti-CL | CL |
| 30% MNIST | 9.19 | 9.28 | 5.46 | 5.60 | 13.17 | <u>4.29</u> | 8.01 | 5.78 | 5.35 |
| 50% MNIST | 3.36 | 5.21 | 2.53 | 3.96 | 4.21 | <u>2.05</u> | 4.10 | 4.11 | 2.96 |
| 100% MNIST | 1.67 | 2.53 | 1.32 | 1.96 | 1.78 | <u>1.17</u> | 1.98 | 1.79 | 1.32 |

| Uncertainty | Baseline | Reorder | | Subsets | | | Weights | | |
|-------------|----------|---------|-------------|---------|---------|-------------|---------|---------|-------------|
| | | Anti-CL | CL | Random | Anti-CL | CL | Random | Anti-CL | CL |
| 30% MNIST | 9.19 | 8.94 | 4.42 | 5.60 | 8.85 | <u>3.69</u> | 8.01 | 8.50 | 5.62 |
| 50% MNIST | 3.36 | 3.23 | 3.04 | 3.96 | 4.21 | <u>2.15</u> | 4.10 | 4.77 | 3.21 |
| 100% MNIST | 1.67 | 2.29 | 1.45 | 1.81 | 2.02 | <u>1.17</u> | 1.99 | 1.66 | 1.33 |

TABLE II: Fracture classification results over 10 runs: mean F_1 -score. The highlighted indices in bold correspond to the best metric per curriculum method. The underlined values correspond to the best metric per scenario, *i.e.* 3-class (type-A or type-B and non-fracture) and 7-class (fracture subtypes and non-fracture) classification.

| Prior knowledge | Baseline | Reorder | | Subsets | | | Weights | | |
|-----------------|----------|---------|--------------|---------|---------|--------------|---------|---------|--------------|
| | | Anti-CL | CL | Random | Anti-CL | CL | Random | Anti-CL | CL |
| 7-class | 56.62 | 34.56 | 68.93 | 58.90 | 50.89 | 66.50 | 58.26 | 55.20 | 64.65 |
| 3-class | 81.71 | 60.46 | 86.23 | 80.82 | 75.64 | 84.69 | 80.66 | 75.33 | 85.66 |

| Uncertainty | Baseline | Reorder | | Subsets | | | Weights | | |
|-------------|----------|---------|--------------|---------|---------|--------------|---------|---------|--------------|
| | | Anti-CL | CL | Random | Anti-CL | CL | Random | Anti-CL | CL |
| 7-class | 56.62 | 61.29 | 64.70 | 58.90 | 62.06 | <u>65.51</u> | 58.26 | 58.29 | 62.29 |
| 3-class | 81.71 | 82.48 | 84.38 | 80.82 | 82.79 | <u>84.90</u> | 80.66 | 82.69 | 82.96 |

size. For the remaining experiments, we employ MNIST, as a controlled environment, to investigate such challenging scenarios. In the third series, we evaluate the classification performance when training with limited amounts of data. In the fourth series, we present the results that deal with class-imbalance. Finally, in our last series of experiments, we discuss and show the performance under the presence of label noise.

V. RESULTS

A. Prior knowledge-driven CL

We evaluated the performance of the classifier with our data scheduler and verified that establishing a curriculum based on prior knowledge is a good and suitable option to improve classification performance. Results for digit recognition are summarized in Table I-top, and for proximal femur fracture in Table II-top. We found that the three variants helped to improve the performance of the two datasets. In contrast with the anti-CL approach, accuracy was increased with respect to the baseline.

For MNIST, we found that training starting with an easy subset, and gradually increasing the subset by adding more difficult samples was the best strategy for the three scenarios as shown in Fig. 3-a. A comparable improvement with respect to the baseline was found when the decay of Eq. (9) was

introduced in reorder strategy and sampling with replacement was performed instead.

For fracture classification, the F_1 -score for 7-class was improved up to 15% compared to the baseline. This score is comparable to state-of-the-art results [17] and experienced trauma surgeons [23]. Although related works report results for binary classification (fracture/no fracture), we are not aware of other teams doing fine-grained multi-class fracture classification. In this case, the best method was reordering the whole training set. We hypothesize that by reordering, we improve diversity by including the more challenging fine-grained fractures classification task than employing subsets of the data. Furthermore, as specified in Subsection IV-B, the CNN for fracture classification was pretrained, whereas for digit recognition the CNN was trained from scratch. From the results in Table II, we can say that our method is compatible with transfer learning.

B. Uncertainty-driven CL

Here, assuming lack of prior knowledge, we confirmed that uncertainty estimation can guide the data scheduling. Results are presented in Table I-bottom and Table II-bottom for MNIST and fractures, respectively. For digit classification, the error rate was reduced up to 30%, see Fig. 3-b. For the fine-grained 7-class proximal femur fractures classification, the F_1 -score was improved up to 16% compared to the

TABLE III: Comparison of curriculum strategies driven by prior knowledge and uncertainty, under class-imbalance and label noise for the MNIST dataset. Mean error rate (%). The highlighted values in bold correspond to the best strategy per scenario.

| | Baseline | Reorder | | Subsets | | Weights | |
|-----------------|----------|----------|-------------|-------------|-------------|----------|-------------|
| | | Prior K. | Uncertainty | Prior K. | Uncertainty | Prior K. | Uncertainty |
| Class-imbalance | 2.53 | 2.08 | 2.05 | 1.79 | 2.08 | 2.31 | 2.22 |
| Label Noise | 9.46 | 8.76 | 8.42 | 8.28 | 7.24 | 8.49 | 5.42 |

baseline. In this case, we found that weighting the samples was not as beneficial as reordering or sampling subsets. The anti-CL approach improved in some cases the classification performance with respect to baseline, but not in a consistent way as the CL approach did.

C. Limited amounts of data

Table I shows the digit recognition performance when restricting the amount of training data to 30% and 50%. When employing our curriculum framework, the error rate for digit classification is reduced in all cases. We found that employing subsets in the first epochs based on uncertainty was the best strategy. Moreover, the effect of our curriculum approach was more evident on the more challenging scenario. The error rate was reduced by up to 59% training with only 30% of the data. Interestingly, we found that when training with only 30% of data, the use of random subsets also reduced the error rate. This behaviour goes along with some findings about training with partial data [44].

D. Class-imbalance

We evaluated our proposed curriculum method in a controlled experiment under class-imbalance with the MNIST dataset. Specifically, the number of examples of two classes (digits 1 and 7) are limited to 30% of the available cases. Results in Table III show that our approach can cope with class-imbalance and improved over the baseline result. Similar to the experiment with limited amount of data, the use of high-priority subsets, selected based on prior knowledge or uncertainty, was the best approach. The subsets approach reduced the error rate from 2.53% to 1.79%.

E. Noisy labels

Using MNIST and a controlled setting, we corrupted a randomly selected 30% of random training labels by assigning to them the subsequent label digit, *i.e.* zeroes become ones, ones become twos, *etc.* Table III reports the mean error rate (%) when evaluating the digit classification. We found that all the variants of our unified CL framework were effective to deal with noisy labels and beat the baseline. In this case, prior knowledge was not as beneficial as the estimation of model prediction uncertainty. The best variant was using uncertainty to weight the classification loss, reducing the error rate by 43%. The fact that uncertainty performed better than prior knowledge was expected, since noise may affect individual samples and not entire classes. It is more reasonable to use

a scoring function that independently affects the samples. Moreover, although reordering and subsets presented all the samples at convergence, weighting seemed to be the only strategy to remove or reduce the influence of the flawed labels.

VI. DISCUSSION

In this work, we bring together several ideas from the literature into a unified CL framework. We experimentally demonstrate the effectiveness of ranking and scheduling training data for multi-class classification, under demanding scenarios such as class-imbalance, limited amounts of data and noisy annotations. We also show its benefits on a clinical dataset that presents the above-mentioned challenges, namely classification of proximal femur fractures.

Our CL framework is compatible with any architecture and stochastic gradient descent training. It only requires the reordering step at the beginning of each epoch. Since the order is pre-computed, no added complexity is introduced for this variant. This complexity slightly increases in the case of subsets. Inspired by classical CL, we leveraged prior knowledge to define the data scheduling elements. In our formulation, it is straightforward to define as it only requires a scalar value per class. In case of multiple experts annotating the dataset, this knowledge can be derived from their intra- or inter-expert variability, or by asking the experts about the perceived difficulty of each class. One limitation of this approach is that the use of prior knowledge at the class level may be less informative for the CNN than at sample level.

When prior knowledge is not available, we have shown that uncertainty can be used to guide the optimization. We used MC to estimate uncertainty. This has the advantage of not requiring any change in the CNN architecture, but it is computationally demanding. Indeed, the training time is doubled in this variant. Instead, one could investigate the use of a Dirichlet distribution to parametrize the output of the network. Then, the behavior of such predictor could be interpreted from an evidential reasoning perspective, such as in subjective logic [45], [46]. We restricted our study to the predictive entropy of the model, which includes both aleatoric and epistemic uncertainty. We reckon that assessing separately each of the types of uncertainty could be advantageous for some applications. Moreover, if computational issues are not a problem, uncertainty does not only rank at the class but at the sample level. This scoring function is more appropriate for noisy annotations, since noise may affect individual samples and not entire classes. We believe that there is research interest on the definition of the scoring function. Therefore, we plan

to investigate the CNN behaviour when using prior knowledge alternatives at sample level, rather than at class level.

We evaluated three variants of our unified framework that consisted of reordering the whole training set, sampling subsets of data, or individually weighting training samples. The reordering and subsets performances are very similar but if the dataset is too complex (fractures) it seems better to keep the entire training set. We found similar performance when the curriculum probabilities were decayed towards a uniform distribution [18] or maintained stable in our reorder and weights variants. Regarding the latter, we have proposed a simple and effective weighting scheme. In future work, we plan to explore other weighting strategies, e.g. the focal loss [47], which is well suited for class-imbalance scenarios, and large margin loss [48], which has been shown beneficial under limited amounts of data and when noisy labels are present.

VII. CONCLUSIONS

In this work we have presented a unified CL framework for multi-class classification. We have identified common scheduling elements in the literature and presented them together in our approach. We have proposed two types of ranking functions to prioritize training data: prior knowledge and uncertainty. In controlled experiments with the MNIST dataset, we have shown that the proposed method is effective for datasets with class-imbalance, limited or noisy annotations. From our experiments, we can conclude that for datasets of limited size or under the presence of class-imbalance, the use of the subsets variant can lead to an improved classification performance. One can either exploit prior knowledge to achieve a better performance, or if the computational cost is not an issue, leverage uncertainty. In the case of unreliable labels, we found that the more advantageous approach is the combination of weights with uncertainty. Finally, we have validated the benefits of our approach on a clinical dataset of proximal femur fractures classification. We reached a performance comparable to state-of-the-art and experienced trauma surgeons.

REFERENCES

- [1] H. Shin, H. R. Roth, M. Gao, L. Lu, Z. Xu, I. Nogues, J. Yao, D. Mollura, and R. M. Summers, "Deep convolutional neural networks for computer-aided detection: CNN architectures, dataset characteristics and transfer learning," *IEEE Transactions on Medical Imaging*, vol. 35, no. 5, pp. 1285–1298, 2016.
- [2] D. Shen, G. Wu, and H.-I. Suk, "Deep learning in medical image analysis," *Annual Review of Biomedical Engineering*, vol. 19, no. 1, pp. 221–248, 2017, pMID: 28301734. [Online]. Available: <https://doi.org/10.1146/annurev-bioeng-071516-044442>
- [3] E. Gibson, W. Li, C. Sudre, L. Fidon, D. I. Shaker, G. Wang, Z. Eaton-Rosen, R. Gray, T. Doel, Y. Hu, T. Whyntie, P. Nachev, M. Modat, D. C. Barratt, S. Ourselin, M. J. Cardoso, and T. Vercauteren, "NiftyNet: a deep-learning platform for medical imaging," *Computer Methods and Programs in Biomedicine*, vol. 158, pp. 113 – 122, 2018. [Online]. Available: <http://www.sciencedirect.com/science/article/pii/S0169260717311823>
- [4] I. Bonavita, X. Rafael-Palou, M. Ceresa, G. Piella, V. Ribas, and M. A. Gonzalez Ballester, "Integration of convolutional neural networks for pulmonary nodule malignancy assessment in a lung cancer classification pipeline," *Computer Methods and Programs in Biomedicine*, vol. 185, p. 105172, 2020. [Online]. Available: <http://www.sciencedirect.com/science/article/pii/S0169260719300975>
- [5] O. Bernard, A. Lalande, C. Zotti, F. Cervenansky, X. Yang, P. Heng, I. Cetin, K. Lekadir, O. Camara, M. A. Gonzalez Ballester, G. Sanroma, S. Napel, S. Petersen, G. Tziritis, E. Grinias, M. Khened, V. A. Kollerathu, G. Krishnamurthi, M. Roh, X. Pennec, M. Sermesant, F. Isensee, P. Jger, K. H. Maier-Hein, P. M. Full, I. Wolf, S. Engelhardt, C. F. Baumgartner, L. M. Koch, J. M. Wolterink, I. Igum, Y. Jang, Y. Hong, J. Patravali, S. Jain, O. Humbert, and P. Jodoin, "Deep learning techniques for automatic mri cardiac multi-structures segmentation and diagnosis: Is the problem solved?" *IEEE Transactions on Medical Imaging*, vol. 37, no. 11, pp. 2514–2525, 2018.
- [6] A. Krizhevsky, I. Sutskever, and G. E. Hinton, "Imagenet classification with deep convolutional neural networks," in *Advances in Neural Information Processing Systems*, 2012, pp. 1097–1105.
- [7] J. Zhou, Z. Li, W. Zhi, B. Liang, D. Moses, and L. Dawes, "Using convolutional neural networks and transfer learning for bone age classification," in *2017 International Conference on Digital Image Computing: Techniques and Applications (DICTA)*. IEEE, 2017, pp. 1–6.
- [8] H. Shang, Z. Sun, W. Yang, X. Fu, H. Zheng, J. Chang, and J. Huang, "Leveraging other datasets for medical imaging classification: Evaluation of transfer, multi-task and semi-supervised learning," in *Medical Image Computing and Computer Assisted Intervention – MICCAI 2019*, D. Shen, T. Liu, T. M. Peters, L. H. Staib, C. Essert, S. Zhou, P.-T. Yap, and A. Khan, Eds. Cham: Springer International Publishing, 2019, pp. 431–439.
- [9] C. N. Vasconcelos and B. N. Vasconcelos, "Increasing deep learning melanoma classification by classical and expert knowledge based image transforms," *CoRR*, abs/1702.07025, vol. 1, 2017.
- [10] H. Su, X. Shi, J. Cai, and L. Yang, "Local and global consistency regularized mean teacher for semi-supervised nuclei classification," in *Medical Image Computing and Computer Assisted Intervention – MICCAI 2019*, D. Shen, T. Liu, T. M. Peters, L. H. Staib, C. Essert, S. Zhou, P.-T. Yap, and A. Khan, Eds. Cham: Springer International Publishing, 2019, pp. 559–567.
- [11] A. G. Roy, S. Conjeti, D. Sheet, A. Katouzian, N. Navab, and C. Wachinger, "Error corrective boosting for learning fully convolutional networks with limited data," in *International Conference on Medical Image Computing and Computer-Assisted Intervention*. Springer, 2017, pp. 231–239.
- [12] C. Xue, Q. Dou, X. Shi, H. Chen, and P.-A. Heng, "Robust learning at noisy labeled medical images: applied to skin lesion classification," in *2019 IEEE 16th International Symposium on Biomedical Imaging (ISBI 2019)*. IEEE, 2019, pp. 1280–1283.
- [13] A. Smailagic, P. Costa, H. Y. Noh, D. Walawalkar, K. Khandelwal, A. Galdran, M. Mirshekari, J. Fagert, S. Xu, P. Zhang *et al.*, "Medal: Accurate and robust deep active learning for medical image analysis," in *2018 17th IEEE International Conference on Machine Learning and Applications (ICMLA)*. IEEE, 2018, pp. 481–488.
- [14] Y. Tang, X. Wang, A. P. Harrison, L. Lu, J. Xiao, and R. M. Summers, "Attention-guided curriculum learning for weakly supervised classification and localization of thoracic diseases on chest radiographs," in *Machine Learning in Medical Imaging*, Y. Shi, H.-I. Suk, and M. Liu, Eds. Cham: Springer International Publishing, 2018, pp. 249–258.
- [15] J. Yang, X. Wu, J. Liang, X. Sun, M. Cheng, P. L. Rosin, and L. Wang, "Self-paced balance learning for clinical skin disease recognition," *IEEE Transactions on Neural Networks and Learning Systems*, pp. 1–15, 2019.
- [16] G. Maicas, A. P. Bradley, J. C. Nascimento, I. Reid, and G. Carneiro, "Training medical image analysis systems like radiologists," in *International Conference on Medical Image Computing and Computer-Assisted Intervention*. Springer, 2018, pp. 546–554.
- [17] A. Jiménez-Sánchez, D. Mateus, S. Kirchhoff, C. Kirchhoff, P. Biberthaler, N. Navab, M. A. González Ballester, and G. Piella, "Medical-based deep curriculum learning for improved fracture classification," in *Medical Image Computing and Computer Assisted Intervention – MICCAI 2019*, D. Shen, T. Liu, T. M. Peters, L. H. Staib, C. Essert, S. Zhou, P.-T. Yap, and A. Khan, Eds. Cham: Springer International Publishing, 2019, pp. 694–702.
- [18] Y. Bengio, J. Louradour, R. Collobert, and J. Weston, "Curriculum learning," in *Proceedings of the 26th International Conference on Machine Learning*, ser. ICML 2009. New York, NY, USA: ACM, 2009, pp. 41–48.
- [19] M. P. Kumar, B. Packer, and D. Koller, "Self-paced learning for latent variable models," in *Advances in Neural Information Processing Systems* 23, J. D. Lafferty, C. K. I. Williams, J. Shawe-Taylor, R. S. Zemel, and A. Culotta, Eds. Curran Associates, Inc., 2010, pp. 1189–1197. [Online]. Available: <http://papers.nips.cc/paper/3923-self-paced-learning-for-latent-variable-models.pdf>

- [20] M. Havaei, N. Guizard, N. Chapados, and Y. Bengio, "Hemis: Hetero-modal image segmentation," in *Medical Image Computing and Computer-Assisted Intervention – MICCAI 2016*, S. Ourselin, L. Joskowicz, M. R. Sabuncu, G. Unal, and W. Wells, Eds. Cham: Springer International Publishing, 2016, pp. 469–477.
- [21] A. Jesson, N. Guizard, S. H. Ghalehjehg, D. Goblot, F. Soudan, and N. Chapados, "CASED: Curriculum adaptive sampling for extreme data imbalance," in *Medical Image Computing and Computer Assisted Intervention – MICCAI 2017*, M. Descoteaux, L. Maier-Hein, A. Franz, P. Jannin, D. L. Collins, and S. Duchesne, Eds. Cham: Springer International Publishing, 2017, pp. 639–646.
- [22] H. Kervadec, J. Dolz, É. Granger, and I. Ben Ayed, "Curriculum semi-supervised segmentation," in *Medical Image Computing and Computer Assisted Intervention – MICCAI 2019*, D. Shen, T. Liu, T. M. Peters, L. H. Staib, C. Essert, S. Zhou, P.-T. Yap, and A. Khan, Eds. Cham: Springer International Publishing, 2019, pp. 568–576.
- [23] D. van Embden, S. Rhemrev, S. Meylaerts, and G. Roukema, "The comparison of two classifications for trochanteric femur fractures: The AO/ASIF classification and the jensen classification," *Injury*, vol. 41, no. 4, pp. 377–381, apr 2010. [Online]. Available: <https://doi.org/10.1016/j.injury.2009.10.007>
- [24] Y. Gal and Z. Ghahramani, "Dropout as a Bayesian Approximation: Representing Model Uncertainty in Deep Learning," in *Proceedings of The 33rd International Conference on Machine Learning*, ser. Proceedings of Machine Learning Research, M. F. Balcan and K. Q. Weinberger, Eds., vol. 48. New York, New York, USA: PMLR, 20–22 Jun 2016, pp. 1050–1059. [Online]. Available: <http://proceedings.mlr.press/v48/gal16.html>
- [25] J. Wu, S. Ruan, C. Lian, S. Mutic, M. A. Anastasio, and H. Li, "Active learning with noise modeling for medical image annotation," in *2018 IEEE 15th International Symposium on Biomedical Imaging (ISBI 2018)*, April 2018, pp. 298–301.
- [26] M. A. Badgeley, J. R. Zech, L. Oakden-Rayner, B. S. Glicksberg, M. Liu, W. Gale, M. V. McConnell, B. Percha, T. M. Snyder, and J. T. Dudley, "Deep learning predicts hip fracture using confounding patient and healthcare variables," *npj Digital Medicine*, vol. 2, no. 1, Apr. 2019. [Online]. Available: <https://doi.org/10.1038/s41746-019-0105-1>
- [27] C.-T. Cheng, T.-Y. Ho, T.-Y. Lee, C.-C. Chang, C.-C. Chou, C.-C. Chen, I.-F. Chung, and C.-H. Liao, "Application of a deep learning algorithm for detection and visualization of hip fractures on plain pelvic radiographs," *European Radiology*, vol. 29, no. 10, pp. 5469–5477, Oct 2019. [Online]. Available: <https://doi.org/10.1007/s00330-019-06167-y>
- [28] Y. Wang, L. Lu, C.-T. Cheng, D. Jin, A. P. Harrison, J. Xiao, C.-H. Liao, and S. Miao, "Weakly supervised universal fracture detection in pelvic x-rays," in *Medical Image Computing and Computer Assisted Intervention – MICCAI 2019*, D. Shen, T. Liu, T. M. Peters, L. H. Staib, C. Essert, S. Zhou, P.-T. Yap, and A. Khan, Eds. Cham: Springer International Publishing, 2019, pp. 459–467.
- [29] A. Kazi, S. Albarqouni, A. J. Sanchez, S. Kirchhoff, P. Biberthaler, N. Navab, and D. Mateus, "Automatic classification of proximal femur fractures based on attention models," in *Machine Learning in Medical Imaging*, Q. Wang, Y. Shi, H.-I. Suk, and K. Suzuki, Eds. Cham: Springer International Publishing, 2017, pp. 70–78.
- [30] A. Jiménez-Sánchez, A. Kazi, S. Albarqouni, C. Kirchhoff, P. Biberthaler, N. Navab, S. Kirchhoff, and D. Mateus, "Precise proximal femur fracture classification for interactive training and surgical planning," *International Journal of Computer Assisted Radiology and Surgery*, vol. 15, no. 5, pp. 847–857, Apr. 2020. [Online]. Available: <https://doi.org/10.1007/s11548-020-02150-x>
- [31] T. Urakawa, Y. Tanaka, S. Goto, H. Matsuzawa, K. Watanabe, and N. Endo, "Detecting intertrochanteric hip fractures with orthopedist-level accuracy using a deep convolutional neural network," *Skeletal Radiology*, vol. 48, no. 2, pp. 239–244, Feb 2019. [Online]. Available: <https://doi.org/10.1007/s00256-018-3016-3>
- [32] E. Meinberg, J. Agel, C. Roberts, M. Karam, and J. Kellam, "Fracture and dislocation classification compendium—2018," *Journal of Orthopaedic Trauma*, vol. 32, pp. S1–S10, Jan. 2018.
- [33] Y. Wang, W. Gan, J. Yang, W. Wu, and J. Yan, "Dynamic curriculum learning for imbalanced data classification," in *The IEEE International Conference on Computer Vision (ICCV)*, October 2019.
- [34] K. A. Hallgren, "Computing inter-rater reliability for observational data: an overview and tutorial," *Tutorials in quantitative methods for psychology*, vol. 8, no. 1, p. 23, 2012.
- [35] Y. Li, L. Liu, and R. T. Tan, "Certainty-driven consistency loss for semi-supervised learning," *CoRR*, vol. abs/1901.05657, 2019. [Online]. Available: <http://arxiv.org/abs/1901.05657>
- [36] C. E. Shannon, "A mathematical theory of communication," *Bell system technical journal*, vol. 27, no. 3, pp. 379–423, 1948.
- [37] F. C. Ghesu, B. Georgescu, E. Gibson, S. Guendel, M. K. Kalra, R. Singh, S. R. Digumarthy, S. Grbic, and D. Comaniciu, "Quantifying and leveraging classification uncertainty for chest radiograph assessment," in *Medical Image Computing and Computer Assisted Intervention – MICCAI 2019*, D. Shen, T. Liu, T. M. Peters, L. H. Staib, C. Essert, S. Zhou, P.-T. Yap, and A. Khan, Eds. Cham: Springer International Publishing, 2019, pp. 676–684.
- [38] G. Hacohen and D. Weinshall, "On the power of curriculum learning in training deep networks," *arXiv preprint arXiv:1904.03626*, 2019.
- [39] Y. Freund, R. Schapire, and N. Abe, "A short introduction to boosting," *Journal-Japanese Society For Artificial Intelligence*, vol. 14, no. 771–780, p. 1612, 1999.
- [40] J. T. Springenberg, A. Dosovitskiy, T. Brox, and M. Riedmiller, "Striving for simplicity: The all convolutional net," *arXiv preprint arXiv:1412.6806*, 2014.
- [41] S. Laine and T. Aila, "Temporal ensembling for semi-supervised learning," in *International Conference on Learning Representations*, 2017. [Online]. Available: <https://openreview.net/pdf?id=BJ6oOfqge>
- [42] K. He, X. Zhang, S. Ren, and J. Sun, "Deep residual learning for image recognition," *2016 IEEE Conference on Computer Vision and Pattern Recognition (CVPR)*, pp. 770–778, 2016.
- [43] A. Jiménez-Sánchez, A. Kazi, S. Albarqouni, C. Kirchhoff, P. Biberthaler, N. Navab, D. Mateus, and S. Kirchhoff, "Towards an interactive and interpretable CAD system to support proximal femur fracture classification," *CoRR*, vol. abs/1902.01338v1, 2019. [Online]. Available: <http://arxiv.org/abs/1902.01338v1>
- [44] M. N. Mermer and M. F. Amasyali, "Training with growing sets: A simple alternative to curriculum learning and self paced learning," 2018. [Online]. Available: <https://openreview.net/forum?id=SJ1fQYICZ>
- [45] M. Sensoy, L. Kaplan, and M. Kandemir, "Evidential deep learning to quantify classification uncertainty," in *Advances in Neural Information Processing Systems 31*, S. Bengio, H. Wallach, H. Larochelle, K. Grauman, N. Cesa-Bianchi, and R. Garnett, Eds. Curran Associates, Inc., 2018, pp. 3179–3189. [Online]. Available: <http://papers.nips.cc/paper/7580-evidential-deep-learning-to-quantify-classification-uncertainty.pdf>
- [46] A. Jøsang, *Subjective Logic: A Formalism for Reasoning Under Uncertainty*, 1st ed. Springer, 2018.
- [47] T.-Y. Lin, P. Goyal, R. Girshick, K. He, and P. Dollár, "Focal loss for dense object detection," in *Proceedings of the IEEE International Conference on Computer Vision*, 2017, pp. 2980–2988.
- [48] G. Elsayed, D. Krishnan, H. Mobahi, K. Regan, and S. Bengio, "Large margin deep networks for classification," in *Advances in Neural Information Processing Systems*, 2018, pp. 842–852.